ELSEVIER

Thermochimica Acta 311 (1998) 105–111

thermochimica acta

Thermal analysis of branched GAP

H.T. Feng, K.J. Mintz, R.A. Augsten, D.E.G. Jones*

Canadian Explosives Research Laboratory, 555 Booth St, Ottawa K1A 0G1, Canada

Received 29 May 1997; received in revised form 14 October 1997; accepted 26 October 1997

Abstract

Branched glycidyl azide polymer (B-GAP) is used in propellant composition as a binder. The thermal properties of B-GAP are therefore of interest. This paper mainly deals with a study of the thermal decomposition of B-GAP using thermal analysis, including DSC, TGA and ARC. The variable heating rate and isothermal techniques were used for obtaining kinetic results for B-GAP. © Minister of Natural Resources Canada, 1998

Keywords: ARC; Branched glycidyl azide polymer (B-GAP); DSC; Kinetics; TGA

1. Introduction

Ammonium perchlorate (AP) has been replaced partially or wholly by ammonium nitrate (AN) in rocket propellant formulations for economy and to improve vulnerability of the propellant. But AN is less energetic than AP. In order to increase the power of a propellant containing AN, other ingredients which have energetic properties should be added. Glycidyl azide polymer (GAP) is an energetic binder which has been used for this purpose.

GAP was originally developed as an energetic binder for composite propellants. A number of papers have been published to describe the properties of GAP [1–3]. The linear chain species is called GAPDIOL. GAPTRIOL and branched GAP (B-GAP) are non-linear polymers which not only have the advantage of forming a more rigid binder network than that of GAPDIOL, when cured, but also of supplying more energy from their combustion [4–6]. The structures of GAPTRIOL and B-GAP are shown in Fig. 1. The thermal properties of GAPTRIOL were described in Ref. [7]. This paper describes the thermal properties of B-GAP and these properties are compared with those of GAPTRIOL.

2. Experimental

B-GAP was obtained from the Defence Research Establishment at Valcartier, Quebec. The sample is a viscous, dark brown liquid with a humidity 0.03%, viscosity (25°C) 23.3 Pa s and an OH equivalent weight of 1697 and was used as obtained.

A TA 2100 Thermal Analyst System with 2910 DSC and 2590 TGA modules was used with a carrier gas flow of 50 $cm^3\ min^{-1}$. Dry oxygen-free nitrogen was used for both DSC and TGA experiments, and dry air was used for TGA experiments only. Heating rates from 2–10°C min^{-1} were used for DSC and TGA measurements. Isothermal experiments were

*Corresponding author. Tel.: 00 1 613 995 2140; fax: 00 1 613 995 1230.

0040-6031/98/$19.00
PII S0040-6031(97)00431-0

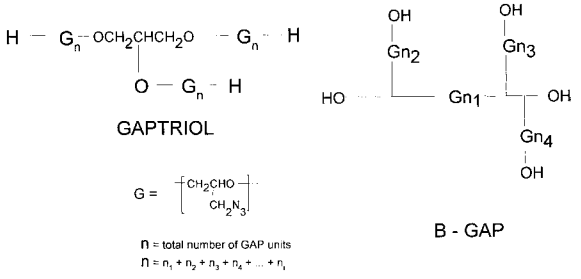

Fig. 1. The structures of GAPTRIOL and B-GAP.

carried out from 190 to 230°C and the data were interpreted using the TA isothermal kinetics software.

The DSC was calibrated for heat flow using a traceable indium standard. For temperature calibration, SRM standards of biphenyl, indium, tin, lead and zinc were used at each heating rate. The calibration was verified and only the value of the heat of fusion for indium within 3% of the literature value was accepted. B-GAP was sealed in glass microampoules. A silver tray with a diameter of 8 mm was wrapped around the microampoule and flattened on the side in contact with the sample platform in the DSC. More details about this technique can be found in Refs. [8,9].

For the TGA 2950 two types of calibrations are required: a mass calibration and a temperature calibration. The standard reference weight was used for mass calibration and the reference weight was checked against a Mettler M3 electrical microbalance with a reproducibility of ±1 μg. For the temperature calibration the Curie Point magnetic method [10] was used. All ferromagnetic substances have a definite transition temperature at which the ferromagnetism disappears and the substances become merely paramagnetic. SRM standards of Permanorm #3, Nickel, Mumetal and Permanorm #5 were used. A small piece of ferromagnetic standard was placed within the field of a magnet so that the resulting magnetic force adds to the gravity effect on the thermobalance. A 10% mass increase in the magnetic field was used in our TGA calibration. At the Curie temperature of the standards the magnetic force vanished and the mass of standards returned to the original. The extrapolated onset temperatures of the mass loss were recorded and compared with reference values [10]. Calibration was done at each heating rate. A platinum sample pan was used for all TGA measurements. Sample size was about 3–4 mg.

The ARC (accelerating rate calorimeter) is a commercial automated adiabatic calorimeter developed by Dow and licensed to CSI (Columbia Scientific Industries), Austin, Texas, for the purpose of assessing the thermal hazard potential of chemicals [11]. The instrument is able to maintain adiabatic conditions provided the rate of temperature rise is not too great, less than about 10°C min^{-1}. Samples of 100–500 mg of B-GAP were placed in lightweight, spherical titanium bombs, which were closed so as to maintain any pressure resulting from vaporisation and decomposition of the sample. Most of the tests were carried out in an inert atmosphere (Ar), but three were performed in air. The standard ARC procedure of 'heat-wait-search' was used; the temperature of the system was raised by 5°C, then kept under adiabatic conditions until thermal transients had disappeared, and finally continued to be held adiabatically while a 'search' was made for the exotherm, which is defined as a self-heating rate (SHR) exceeding 0.02°C min^{-1}. It is important to note that an exotherm cannot be detected in either the 'heat' or 'wait' steps.

3. Results and discussion

3.1. DSC and TGA

The DSC and TGA curves of B-GAP, at 10°C min^{-1}, are compared in Fig. 2. An exotherm with an onset of temperature of 170±4°C and ΔH=2.59±0.15 kJ g^{-1} was observed, compared with the onset temperature of 180±4°C and ΔH= 2.58±0.05 kJ g^{-1} for GAPTRIOL. The exotherm corresponds with the initial mass loss observed in the TGA experiments carried out in nitrogen.

The following description of the kinetic results is based on the *n*th-order rate law:

$$d\alpha/dt = k(1-\alpha)^n$$

and the Arrhenius equation

$$k = Z\exp(E_a/RT)$$

where α is the fraction of sample reacted ($0 \leq \alpha \leq 1$), k the rate constant of the reaction, n the order of the

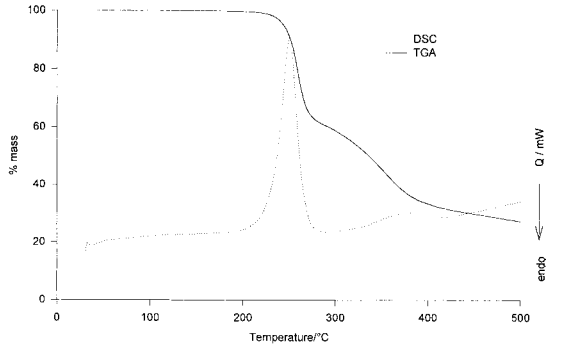

Fig. 2. DSC and TGA (in nitrogen) of B-GAP at β=10 K min^{-1}.

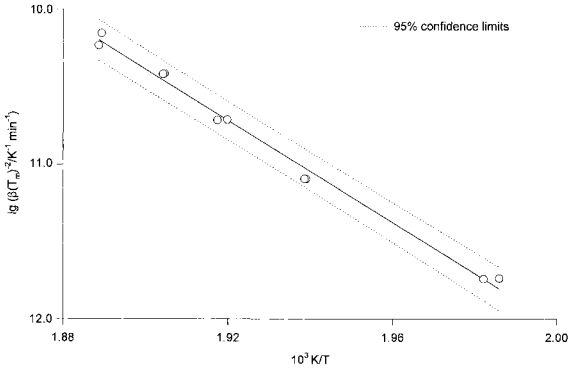

Fig. 3. Arrhenius plot of DSC variable heating rate results for B-GAP.

reaction, E_a the activation energy, and Z the pre-exponential factor in the Arrhenius equation.

For the DSC dynamic measurements, the various heating rate results were analysed by plotting $\lg(\beta/T_m^2)$ against $1/T_m$, where β is the heating rate and T_m the peak temperature, corrected for thermal lag [12]. Fig. 3 shows these results.

Isothermal DSC results are shown in Fig. 4(a). The software package obtained from TA Instruments was used to determine n and k from a plot of $\lg(d\alpha/dt)$ against $\lg(1-\alpha)$. These results are shown in Fig. 4(b). The curvature of the experimental results in Fig. 4(b) suggests that this reaction may not be of first order. An autocatalytic model gives a linear plot, but there is a larger uncertainty in the results from this model because of the software used to obtain these results. Fig. 4(c) shows the plot of $\lg(k/\text{min}^{-1})$ against inverse isothermal temperature, where k is the rate constant for the nth-order model.

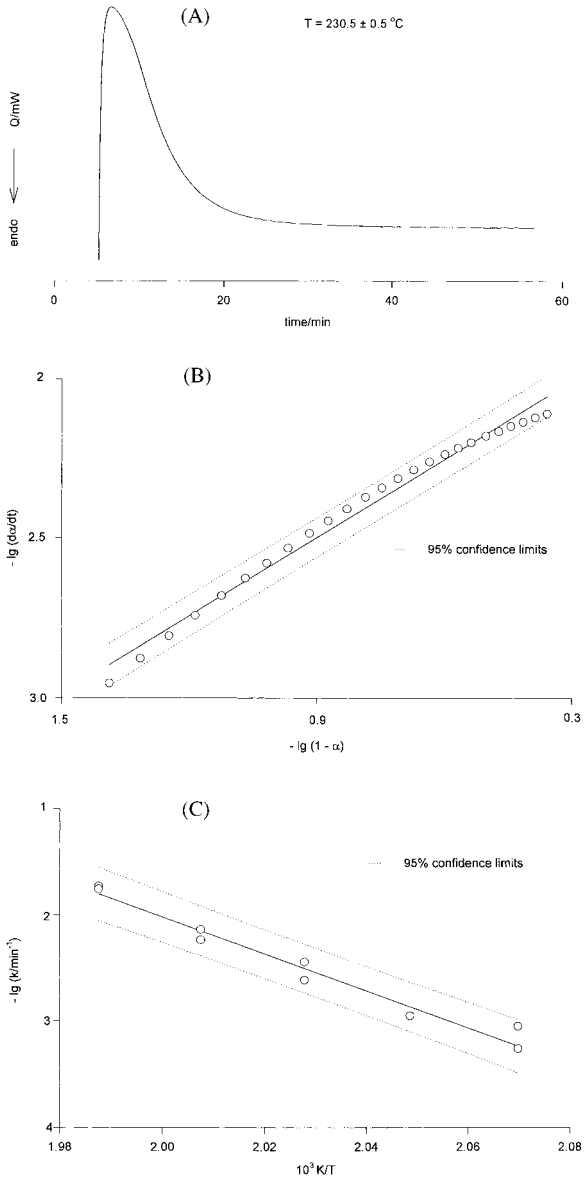

Fig. 4. (a) Isothermal DSC of B-GAP at 230°C, (b) Plot of $\lg(d\alpha/dt)$ vs. $\lg(1-\alpha)$ for data in Fig. 3(a), (c) Arrhenius plot for rate constants obtained from isothermal DSC curves using nth-order model.

The TGA results for B-GAP in nitrogen and air are compared in Fig. 5. About 40% mass loss took place in the first stage which likely corresponds to loss of N_2+H_2 from the repeating units in B-GAP, similar to GAPTRIOL. Higher mass loss than expected (30% based on conversion of azide to cyano group and

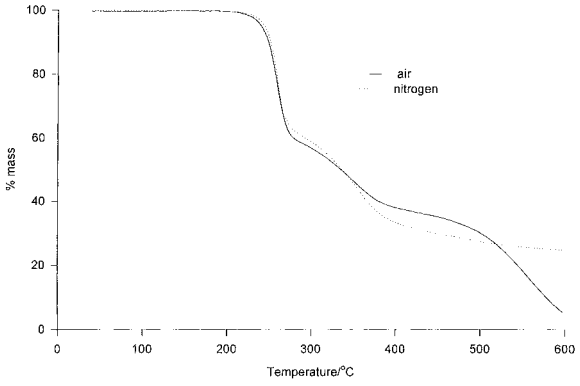

Fig. 5. TGA of B-GAP at β=10 K min^{-1} in air and nitrogen.

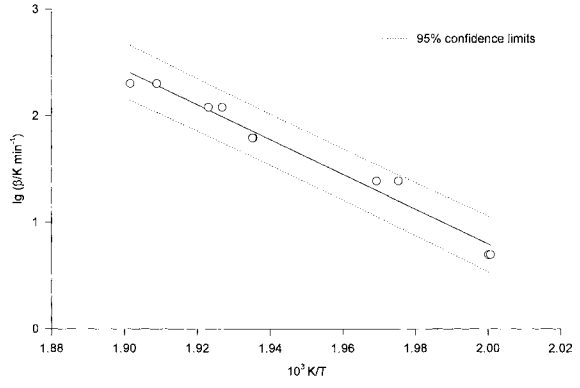

Fig. 6. Fit of lg(β/K min^{-1}) for 10% mass loss in TGA experiments.

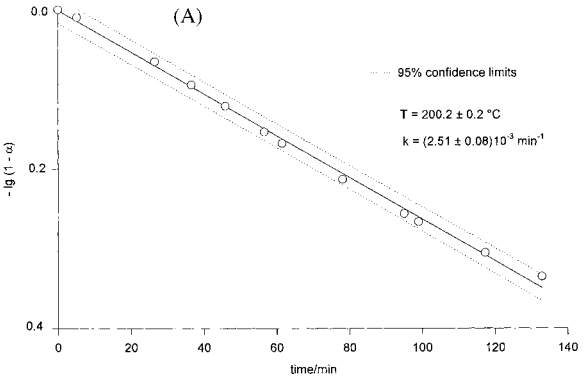

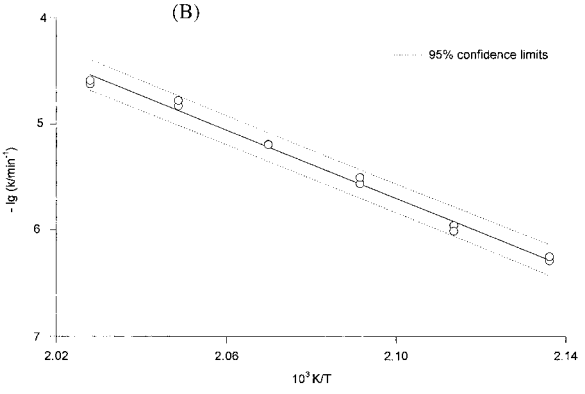

Fig. 7. (a) First-order plot of TGA data at 200.2±0.2°C, R^2=0.996, (b) Arrhenius plot for rate constants obtained from isothermal TGA curves, assuming first-order reaction.

N_2+H_2) suggests that significant decomposition, arising from the second stage reaction, has occurred. The first stage reaction is much faster than the second stage reaction. The first stage reaction was assumed to be of first order. Hence, the second stage reaction is believed to be of higher order. Fig. 6 shows a plot of lg(β/K min^{-1}) against reciprocal temperature at 10% conversion, for the purpose of determining the kinetic parameters [13].

An isothermal study for B-GAP was also performed by TGA. For a first-order reaction, the plot of lg(1−α) against time should give a straight line with slope corresponding to k, the rate constant of reaction. Fig. 7(a) shows these results. Fig. 7(b) shows a plot of lg(k/min^{-1}) against inverse isothermal temperature. The slope of this straight line gives E_a, the activation energy and the intercept is Z, the pre-exponential factor.

After the isothermal DSC experiments, the samples were re-run from room temperature to 500°C at β=10°C min^{-1}. The residual ΔH values appear to decrease with isothermal temperature increase in a linear fashion, but the peak temperature of the reaction did not change significantly. The ΔH for the second reaction showed no significant change. The second reaction is likely from oxidation of the polymer chain and is similar to the ARC results discussed below. The peak temperature obtained from the DTGA curve is about 350°C compared with 370°C obtained from the DSC curve, both at β=10°C min^{-1}. Figs. 2 and 8 show these results.

3.2. ARC

Fig. 9 shows the results of tests carried out on B-GAP in Ar and in air using ARC. At the end of the

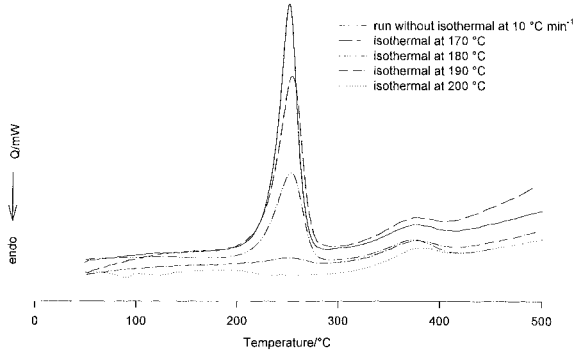

Fig. 8. Variation in residual ΔH after DSC experiments at various isothermal temperatures.

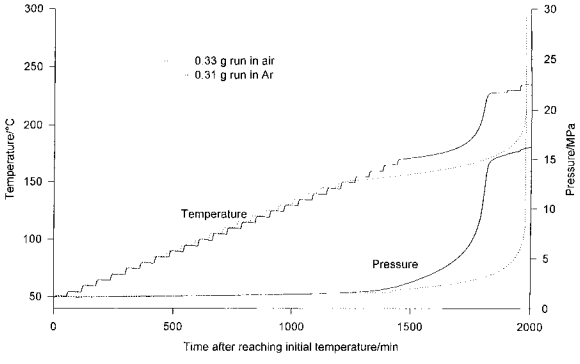

Fig. 9. Accelerating rate calorimeter tests on B-GAP in air and in Ar.

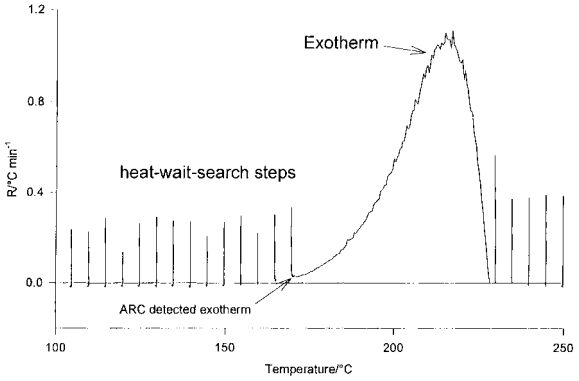

Fig. 10. Self-heating rate of B-GAP in Ar by accelerating rate calorimetry.

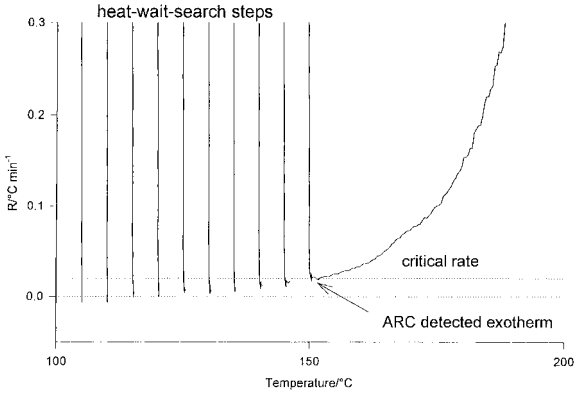

Fig. 11. Self-heating rate of B-GAP in air by accelerating rate calorimetry.

'staircase', the ARC detects the exotherm (SHR>0.02°C min^{-1}) and does not apply any more heat steps until the SHR drops below 0.02°C min^{-1}, i.e. at the end of the exotherm. Fig. 9 clearly shows that the onset temperature is significantly lower in air than in Ar. However, initially the temperature and pressure in the air test did not rise as rapidly, but eventually these increases were so great that the test had to be terminated because of the likelihood of an explosion.

The onset temperature detected by the ARC depends upon the arbitrary value of the critical SHR selected by the operator (usually 0.02°C min^{-1}), based on the sensitivity of the instrument. Fig. 10, in which the data from the Ar trial are plotted as dT/dt vs. T, shows that self-heating started about 10°C before the ARC detected the exotherm. In contrast, the data from the air trial, plotted similarly (Fig. 11), indicate that self-heating started approximately 35°C before the ARC detected the exotherm. The temperature at which self-heating starts should be considered as the 'true' onset temperature.

The concept of an 'onset temperature' has great practical usage for determining a safe temperature for processes and storage. It is, however, a kinetic parameter rather than a thermodynamic one: it can be defined as the temperature just below which the rate of reaction is too small to be detected. For the ARC experiments in Ar, as illustrated in Fig. 10, the onset temperature is reasonably well defined. In contrast, the onset temperature with air (Fig. 11) does not have a well-defined value. Trials carried out under various

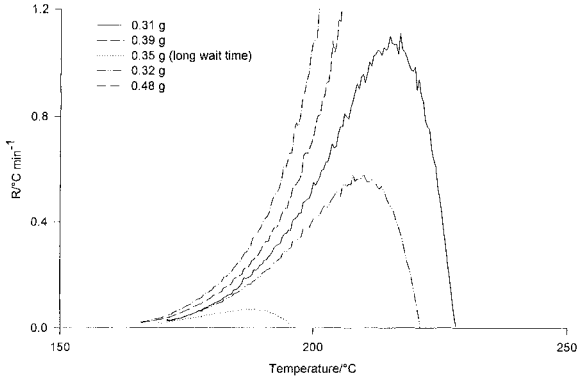

Fig. 12. Accelerating rate calorimetry tests of B-GAP in Ar as a function of sample mass and wait time.

conditions with Ar yielded onset temperatures of 166–171°C (ARC detected) and 157–163°C ('true'); with air, the values ranged from 141–156°C (ARC-detected) and 100–130°C ('true'). The ARC-detected onset temperature is about 30°C below the beginning of the exotherm measured by the DSC, with the true onset even lower. This difference can be attributed to the much larger quantities used in the ARC as well as the ARC being nearly adiabatic.

Trials carried out using different masses of B-GAP (Figs. 12 and 13) indicate that the larger the mass the larger is the exotherm; furthermore, the data suggest that there may be a critical mass above which the sample explodes. Using a long wait time (Fig. 12), i.e. a gradual heating, may allow the material to decompose less vigorously than it otherwise would.

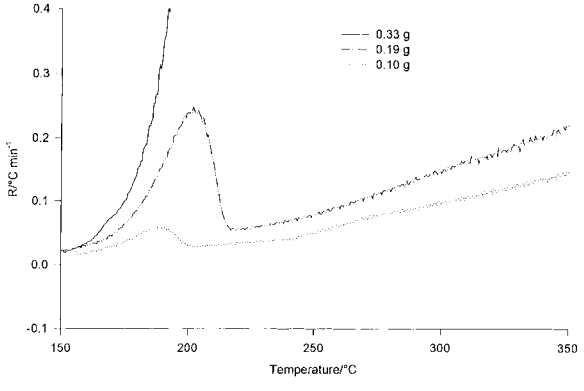

Fig. 13. Self-heating rates of B-GAP in air showing the exotherm due to oxidation.

In contrast to the trials in Ar (Fig. 12) which show a single exotherm, the trials in air (Fig. 13) show a distinct exotherm peak superimposed upon a gradually rising peak. The distinct exotherm is probably due to the generation of nitrogen from the azide part of the molecule (as is the exotherm in the Ar trials); the gradual exotherm may be due to oxidation and degradation of the polymer. The indication that the azide exotherm occurs earlier is probably just due to self-heating from the slow oxidation.

The Arrhenius parameters were obtained by the same method as used previously [7], yielding values, for the trials in Ar, of E_a (178–220 kJ mol^{-1}), lg(Z/min^{-1}) (41–52), and n (0.70–1.28). Despite the variation from trial-to-trial, within each trial, the fit was very good, with $r^2 \sim 0.99$. These values of E_a and lg(Z/min^{-1}) are significantly greater than those obtained in the DSC and TGA work. However, the trial in Ar using 0.33 g B-GAP yielded E_a=132 kJ mol^{-1} and lg(Z/min^{-1})=29, very close to the DSC values. The DSC tests were carried out in microampoules in which necessarily air is incorporated; hence, there may have been some oxidation occurring simultaneously with evolution of nitrogen.

4. Summary

The activation energy and the pre-exponential factor of B-GAP were obtained from four different types of experiment. These results are shown in Table 1. It is found that the values of the activation energy and the pre-exponential factor obtained by different methods agree within the estimate of uncertainty. Similar results for the activation energy and the pre-exponential factor were obtained for GAPTRIOL [7]. From Table 1, it can be seen that the activation energy for B-GAP is lower than that for GAPTRIOL, indicating that B-GAP is more reactive.

The peak temperatures obtained from the derivative of the TGA curve are consistently larger than those obtained from the DSC. The differences in these temperatures are attributed to the difference in the experimental conditions, namely, sample size and open (TGA) and closed (DSC) systems.

Table 1
Comparison of kinetic parameters of B-GAP and GAPTRIOL by various methods

Methods	E_a kJ mol^{-1}		lg(Z/min^{-1})		n
	B-GAP	GAPTRIOL	B-GAP	GAPTRIOL	
DSC (dynamic)	138±4	160	30.74±0.05 [a]	25.04 [a]	[1]
DSC (isothermal)	145±9	178	33.0±2.2	41.0	$0.66_{\text{B-GAP}}$
TGA (dynamic)	136±8 [d]	155	28.57±0.08 [a]	34.92 [a]	[1]
TGA (isothermal)	134±4	—	28.1±1.0	—	[1] [b]
ARC	132 [c] (air)	182 (nitrogen)	29.03	42.15	0.88_{GAPTRIOL}

[a] The reaction was assumed to be of first order.
[b] The reaction was assumed to be of first order based on the linearity of the plot in Fig. 7(a).
[c] The experimental value is mass-dependant. This value is derived from an experiment using 0.33 g of B-GAP.
[d] The uncertainty is derived from the average between 4–15% mass loss.

References

[1] N. Kubota, T. Sonobe, A. Yamamoto, Proc. 19th Annual Conf. of ICT, Combustion and Detonation Phenomena, Fraunhofer Institute, Karlsruhe, Germany, 1988, pp. 1–2.
[2] A.L. Leu, S.M. Shen, B.H. Wu, S.I. Shen, H.C. Yen, G.C. Bai, Proc. 21st Annual Conf. of ICT, Technology of Polymer Compounds and Energetic Materials, Fraunhofer Institute, Karlsruhe, Germany, 1990, pp. 6–10.
[3] Y. Oyumi, Propellants, Explosives and Pyrotechnics 17 (1992) 226.
[4] M.B. Frankel, L.R. Grant, J.E. Flanagan, J. Propulsion Power 8 (1992) 560.
[5] E. Ahad, Proc. 21st Annual Conf. of ICT, Technology of Polymer Compounds and Energetic Material, Fraunhofer Institute, Karlsruhe, Germany, 1990, pp. 5–10.
[6] V.T. Bui, E. Ahad, D. Rheaume, M.P. Raymond, J. of Applied Polymer Science 62 (1996) 27.
[7] D.E.G. Jones, L. Malechaux, R.A. Augsten, Thermochimica Acta 242 (1994) 187.
[8] L.F. Whiting, M.S. Labean, S.S. Eadie, Thermochimica Acta 136 (1988) 231.
[9] D.E.G. Jones, R.A. Augsten, Thermochimica Acta 286 (1996) 355.
[10] ASTM E1582 American Society for Testing and Materials, Philadelphia, PA, USA.
[11] J.C. Tou, L.F. Whiting, Thermochimica Acta 48 (1981) 21.
[12] ASTM E698 American Society for Testing and Materials, Philadelphia, PA, USA.
[13] J.H. Flynn, L.A. Wall, Polymer Letter 19 (1966) 323.